Radical Enhanced Atomic Layer Deposition of Tantalum Oxide

Antti Niskanen,*,† Ulrich Kreissig,‡ Markku Leskelä,† and Mikko Ritala†

Laboratory of Inorganic Chemistry, Department of Chemistry, P.O. Box 55, University of Helsinki, 00014 Helsinki, Finland, and Institute of Ion Beam Physics and Materials Research, Forschungszentrum Rossendorf, P.O. Box 510119, 01314 Dresden, Germany

Received November 7, 2006. Revised Manuscript Received February 5, 2007

Tantalum oxide was deposited by radical enhanced atomic layer deposition using tantalum ethoxide and oxygen radicals. The radicals were produced by dissociating oxygen gas in a remote microwave plasma discharge. Argon was used as the carrier and purge gas. The films were deposited at 150 and 250 °C on glass, silicon, and platinum substrates. Growth rate of the films was 0.19 nm per cycle with a 0.6 s pulse length for tantalum ethoxide and 3 s for oxygen radicals. The films were amorphous according to X-ray diffraction. The densities measured by X-ray reflectivity were between 7.1 and 7.6 g/cm^3 for films grown both at 150 and 250 °C. The dielectric constants were 28 and 36 for films grown on platinum electrodes at 150 and 250 °C, respectively. The leakage current densities at 1 MV/cm electric field were less than 1×10^{-8} A/cm^2 for both deposition temperatures. The effect of water as an additional oxidant was studied at 250 °C. The water was supplied as a separate pulse either right before or after the tantalum ethoxide pulse.

Introduction

Tantalum oxide can be used in a variety of applications because of its good chemical and physical properties. Tantalum oxide is very stable both chemically and thermally and has suitable properties for optic, optoelectronic, and electronic applications. Probably the most studied of these are the electronic applications, where the insulating and dielectric properties of tantalum oxide are utilized.[1−3] The dielectric constant of tantalum oxide is between 22 and 40, depending on the phase. Generally, the dielectric constant is around 22−28 for amorphous tantalum oxide and up to 40 for crystalline phases.[3] Although amorphous tantalum oxide has a relatively high dielectric constant, it suffers from relatively high leakage currents. Nevertheless, the high dielectric constant and relatively easy integration into existing manufacturing processes have made it possible to use tantalum oxide in integrated thin film capacitors and as a dielectric layer in ultra large scale integration (ULSI) dynamic random access memory (DRAM) devices. In earlier DRAM generations, the capacitor dielectric has either been silicon dioxide or a silicon oxide/nitride (ONO) composite. Although the ONO structure was sufficient for 256 Mb DRAMs, modern devices have adopted dielectric materials with higher permittivities, such as Ta_2O_5.[1]

The high permittivity of Ta_2O_5 has also been utilized in low-voltage organic thin film transistor (OTFT) devices.[4] Tantalum oxide has also been used in ion-sensitive field-effect transistors (ISFETs) as an ion-sensing material.[5] ISFETs have been used to measure pH and as ion and biosensors. Tantalum oxide has a refractive index of 2.25 and has been used in optical waveguides and optical coatings. Tantalum oxide is also an ion conductor and has been used in solid-state electrochromic devices.[6]

Tantalum oxide can be deposited by various physical and chemical methods, such as chemical vapor deposition (CVD), sputtering, evaporation, ion-assisted deposition, and the sol−gel method.[3] Atomic layer deposition (ALD) of tantalum oxide has been accomplished with a number of processes utilizing either tantalum halides or organometallic compounds as the tantalum precursor. Probably the most studied process has been $TaCl_5$ and water,[7−10] but several other tantalum precursors have also been used with water: TaI_5,[11,12]

* Corresponding author. E-mail: antti.niskanen@helsinki.fi.
† University of Helsinki.
‡ Forschungszentrum Rossendorf.

(1) Lee, J. Y.; Lai, B. C. In *Handbook of Thin Films Materials*; Nalwa, H. S., Ed.; Academic Press: San Diego, CA, 2002; p 1.
(2) Yoon, D.; Roh, J.; Baik, H. K.; Lee, S. *Crit. Rev. Solid State Mater. Sci.* **2002**, *27*, 143.
(3) Chaneliere, C.; Autran, J. L.; Balland, B.; Devine, R. A. B. *Mater. Sci. Eng., R* **1998**, *22*, 269.
(4) Liang, Y.; Dong, G.; Hu, Y.; Wang, L.; Qiu, Y. *Appl. Phys. Lett.* **2005**, *86*, 132101.
(5) Kwon, D.; Cho, B.; Kim, C.; Sohn, B. *Sens. Actuators, B* **1996**, *34*, 441.
(6) Ritala, M.; Leskelä, M. In *Handbook of Thin Films Materials*; Nalwa, H. S., Ed.; Academic Press: San Diego, CA, 2002; p 103.
(7) Aarik, J.; Aidla, A.; Kukli, K.; Uustare, T. *J. Cryst. Growth* **1994**, *144*, 116.
(8) Kukli, K.; Aarik, J.; Aidla, A.; Kohan, O.; Uustare, T.; Sammelselg, V. *Thin Solid Films* **1995**, *260*, 135.
(9) Aarik, J.; Kukli, K.; Aidla, A.; Pung, L. *Appl. Surf. Sci.* **1996**, *103*, 331.
(10) Kukli, K.; Ritala, M.; Matero, R.; Leskelä, M. *J. Cryst. Growth* **2000**, *212*, 459.
(11) Kukli, K.; Aarik, J.; Aidla, A.; Forsgren, K.; Sundqvist, J.; Hårsta, A.; Uustare, T.; Maendar, H.; Kiisler, A. *Chem. Mater.* **2001**, *13*, 122.
(12) Sundqvist, J.; Hoegberg, H.; Hårsta, A. *Chem. Vap. Deposition* **2003**, *9*, 245.

10.1021/cm0626482 CCC: $37.00
Published on Web 03/30/2007

Table 1. Pulsing Sequences and Growth Rates at 250 °C

	steps						
sequence	1	2	3	4	5	6	growth rate (nm/cycle)
Ta−O	$Ta(OEt)_5$	purge	O	purge			0.19
Ta−H_2O−O	$Ta(OEt)_5$	purge	H_2O	purge	O	purge	0.11
H_2O−Ta−O	H_2O	purge	$Ta(OEt)_5$	purge	O	purge	0.19
Ta−H_2O	$Ta(OEt)_5$	purge	H_2O	purge			0.05

$Ta(OC_2H_5)_5$,[13−15] and tantalum alkylamides.[16] Other oxygen sources have been hydrogen peroxide[11] and molecular oxygen.[12] Also, the reactions between $Ta(OC_2H_5)_5$ and $TaCl_5$ have been used to deposit tantalum oxide without any separate oxygen precursor.[17] Plasma-enhanced ALD has also been used to deposit tantalum oxide from $Ta(OC_2H_5)_5$ and oxygen radicals.[18]

In this work, tantalum oxide is deposited with radical enhanced atomic layer deposition (REALD) from tantalum ethoxide and oxygen radicals. Oxygen radicals are highly reactive species typically generated with a plasma discharge and are widely used in thin film deposition and processing.[19] Because of the high reactivity of oxygen radicals, low deposition temperature and high purity characterize the REALD oxide processes.[20] In REALD, the deposition temperature is limited only by the evaporation and thermal decomposition temperature of the metal-containing precursor. Plasma-enhanced atomic layer deposition (PEALD) is similar to REALD but with the distinction that in PEALD, the growing film is exposed to ion and electron bombardment from the plasma. This may cause film damage and contamination due to ion-bombardment-enhanced decomposition of precursor ligands. In REALD, the plasma is upstream of the substrate and only radicals, not ions or electrons, reach the substrate. REALD has been used to deposit aluminum oxide[20] and metallic copper.[21] PEALD has been utilized more widely, mainly because PEALD equipment has been available commercially for longer. PEALD processes include oxides such as HfO_2,[22,23] ZrO_2,[23−25] Al_2O_3,[26−28] Ga_2O_3,[29] nitrides TaN,[30] TiN,[31−33] and metals Al,[34] Ta, and Ti.[35]

Experimental Section

The growth experiments were carried out in a flow-type ALD-reactor with inert gas valving.[6] The reactor had been modified to incorporate a remote microwave plasma source for radical generation.[21] The reactor operates at 1 mbar pressure. Argon (AGA, 99.98%) was used as the carrier and purge gas and was purified with Aeronex GateKeeper inert gas purifier to decrease the impurity levels below 1 ppb. Tantalum ethoxide (Aldrich, 98%) was used as the tantalum precursor and was evaporated from an open boat at 95 °C inside the reactor. Oxygen radicals, produced from molecular oxygen gas (AGA, 99.999%) by the plasma discharge, were used as the oxygen source. Some experiments utilized water as an additional precursor either before or after the tantalum ethoxide pulse (Table 1). The pulsing sequences will be referred to as Ta−O, H_2O−Ta−O, or Ta−H_2O−O, according to Table 1. The Ta−O sequencing is viewed as the baseline experiment. The growth rate saturation experiments were conducted with this sequencing. The H_2O−Ta−O sequencing was used to study the effects of hydroxylating the surface onto which tantalum ethoxide chemisorbs. The Ta−H_2O−O sequence is a modification of the thermally activated ALD process for tantalum oxide using $Ta(OC_2H_5)_5$ and water[13,14] but with every cycle ending with an additional oxidation step using oxygen radicals. The final oxygen radical pulse may also modify the surface onto which tantalum ethoxide adsorbs at the beginning of the next deposition cycle.

Tantalum oxide was grown on n-type silicon, borosilicate glass, and platinum films evaporated on silicon. Films were deposited at 150 and 250 °C. The tantalum ethoxide and oxygen radical pulse lengths were varied to study the effect on the growth rate. For the oxygen radical pulse length experiments, the tantalum ethoxide pulse length was fixed to 2 s with a 4 s purge period. Similarly, for the tantalum ethoxide pulse length experiments, the oxygen radical pulse length was 7 s with a 3 s purge period. Throughout the experiments, the tantalum ethoxide purge time was twice the corresponding pulse time to allow sufficient removal of the precursor from the gas phase.

The film composition was determined by elastic recoil detection analysis (ERDA) at the Rossendorf 5 MV tandem accelerator. The measurements were performed with 35 MeV Cl^{7+} ions hitting the samples under an angle of 15° relative to the surface. The light recoiled atoms and the scattered chlorine ions were detected by a Bragg ionization chamber under a forward direction of 30°. The H-recoils were detected by a Si-detector that was shielded by a 18 μm thick Al foil against all other particles. Further details of the

(13) Kukli, K.; Ritala, M.; Leskelä, M. *J. Electrochem. Soc.* **1995**, *142*, 1670.
(14) Kukli, K.; Aarik, J.; Aidla, A.; Siimon, H.; Ritala, M.; Leskelä, M. *Appl. Surf. Sci.* **1997**, *112*, 236.
(15) Kwak, J.; Lee, Y.; Choi, B. *Appl. Surf. Sci.* **2004**, *230*, 249.
(16) Hausmann, D. M.; de Rouffignac, P.; Smith, A.; Gordon, R. G.; Monsma, D. *Thin Solid Films* **2003**, *443*, 1.
(17) Kukli, K.; Ritala, M.; Leskelä, M. *Chem. Mater.* **2000**, *12*, 1914.
(18) Song, H.; Lee, C.; Kang, S. *Electrochem. Solid-State Lett.* **2001**, *4*, F13.
(19) Rossnagel, S. M.; Cuomo, J. J.; Westwood, W. D. *Handbook of Plasma Processing Technology—Fundamentals, Etching, Deposition, and Surface Interactions*; Noyes: Park Ridge, NJ, 1990.
(20) Niskanen, A.; Arstila, K.; Ritala, M.; Leskelä, M. *J. Electrochem. Soc.* **2005**, *152*, F90.
(21) Niskanen, A.; Rahtu, A.; Sajavaara, T.; Arstila, K.; Ritala, M.; Leskelä, M. *J. Electrochem. Soc.* **2005**, *152*, G25.
(22) Kim, J.; Kim, S.; Jeon, H.; Cho, M.; Chung, K.; Bae, C. *Appl. Phys. Lett.* **2005**, *87*, 053108.
(23) Endo, K.; Tatsumi, T. *Jpn. J. Appl. Phys. Part 2* **2003**, *42*, L685.
(24) Kim, J. Y.; Kim, S. H.; Seo, H.; Kim, J.; Jeon, H. *Electrochem. Solid-State Lett.* **2005**, *8*, G82.
(25) Yun, S. J.; Lim, J. W.; Lee, J. *Electrochem. Solid-State Lett.* **2004**, *7*, F81.
(26) Ha, S.; Choi, E.; Kim, S.; Sung Roh, J. *Thin Solid Films* **2005**, *476*, 252.
(27) Jeong, C.; Lee, J.; Joo, S. *Jpn. J. Appl. Phys., Part 1* **2001**, *40*, 285.
(28) Lim, J. W.; Yun, S. J. *Electrochem. Solid-State Lett.* **2004**, *7*, F45.
(29) Shan, F. K.; Liu, G. X.; Lee, W. J.; Lee, G. H.; Kim, I. S.; Shin, B. C. *J. Appl. Phys.* **2005**, *98*, 023504.
(30) Furuya, A.; Tsuda, H.; Ogawa, S. *J. Vac. Sci. Technol., B* **2005**, *23*, 979.
(31) Greer, F.; Fraser, D.; Coburn, J. W.; Graves, D. B. *J. Vac. Sci. Technol., A* **2003**, *21*, 96.
(32) Heil, S. B. S.; Langereis, E.; Kemmeren, A.; Roozeboom, F.; van de Sanden, M. C. M.; Kessels, W. M. M. *J. Vac. Sci. Technol., A* ***2005***, 23, L5.
(33) Kim, D.; Kim, Y. J.; Park, J.; Kim, J. H. *Mater. Sci. Eng., C* **2004**, *24*, 289.
(34) Lee, Y. J.; Kang, S. *Electrochem. Solid-State Lett.* **2002**, *5*, C91.
(35) Rossnagel, S. M.; Sherman, A.; Turner, F. *J. Vac. Sci. Technol., B* **2000**, *18*, 2016.

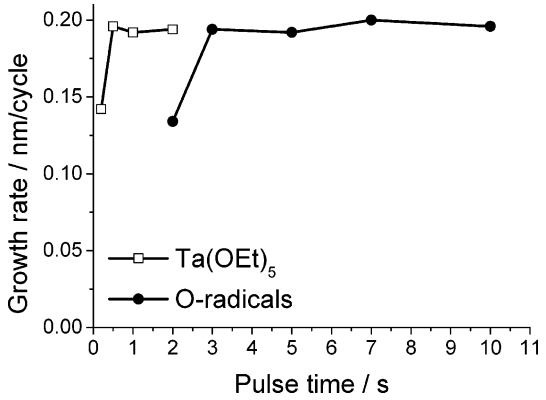

Figure 1. Effect of tantalum ethoxide and oxygen radical pulse lengths on growth rate.

overall experimental setup can be found elsewhere.[36] The energy spectra of recoils and scattered ions were converted into concentration versus depth profiles by means of a computer code[37] using the stopping power data from Ziegler et al.[38]

Film crystallinities were studied with grazing incidence X-ray diffraction (GIXRD), and film thickness, density, and interface roughness were measured using X-ray reflectivity (XRR). Both measurements were conducted with a Bruker AXS D8 Advance diffractometer/reflectometer operated in parallel beam geometry. For thicker films, film thicknesses and refractive indexes were determined by fitting optical reflectance spectra measured within a wavelength range of 370−1100 nm using a Hitachi U-2000 spectrophotometer.[39] The angular range of the XRR measurements was to 1.5° (2θ), with a step size of 0.006°. The measurements were analyzed by fitting a theoretical curve on the measurements using Leptos 1.07 software package by Bruker AXS.

To measure leakage current densities and capacitances of the films, we grew tantalum oxide on evaporated platinum films at 150 and 250 °C. The samples for electrical measurements were deposited using a 1.2 s tantalum ethoxide pulse with a 4 s purge period followed by 10 s oxygen radical pulse. Evaporated aluminum was used as the top electrode. The platinum evaporation was done using an Instrumentti Mattila IM-1992 electron beam evaporator. The aluminum evaporation was done through a shadow mask using an Edwards Auto 306 resistive evaporator. A Keithley 2400 SourceMeter was used for measuring the leakage current densities. Capacitance measurements were done with a HP4284A LCR meter at a frequency of 100 kHz.

Film conformality was studied by depositing films on substrates with patterned trenches and studying the cleaved cross-sections with a Hitachi S-4800 field emission scanning electron microscope (FESEM).

Results and Discussion

The dependence of growth rate on the tantalum ethoxide and oxygen radical pulse lengths was studied at 150 °C with the Ta−O sequencing (Figure 1). The growth rate was found to saturate with 0.6 s tantalum ethoxide pulse length. In the thermally activated tantalum ethoxide−water process, a 0.2 s tantalum ethoxide pulse was found to be sufficient for growth rate saturation at 250 °C.[13] The longer pulse time required in these experiments is probably due to the larger reaction chamber volume used in these experiments: the precursor transport takes longer in the larger volume and thus saturation is reached more slowly. The growth rate was saturated with a 3 s oxygen radical pulse length (Figure 1). The saturated growth rate was 0.195 nm per reaction cycle, and the films grew conformally, as can be seen in the cross-sectional SEM images (Figure 2). The SEM images also show small voids in the trench corers, which are possibly formed during the cleaving of the sample by small-scale adhesion failure. The voids are not seen in a narrower trench, possibly due to greater mechanical support offered by the substrate (Figure 2).

The effect of an additional water pulse was studied at 250 °C. The water pulse was given either before or after the tantalum ethoxide pulse (Table 1). The addition of a water pulse before the tantalum precursor, the H_2O−Ta−O sequence, resulted in the same growth rate as the Ta−O pulsing sequence. In both cases, the chemisorbed tantalum ethoxide is oxidized by oxygen radicals. Pulsing water immediately after tantalum ethoxide, according to the Ta−H_2O−O sequence, resulted in a significantly lower growth rate of 0.11 nm/cycle. This is higher than the growth rate obtained in the same reactor with the thermally activated tantalum ethoxide−water process, 0.05 nm/cycle at 250 °C, even if in both cases the chemisorbed tantalum ethoxide is reacted with water. One possible explanation for this difference is that the oxygen radical pulse in the end of the Ta−H_2O−O sequence increases the number of adsorption sites on which tantalum ethoxide can attach to during the next reaction cycle. Thus, the amount of film grown per cycle would be closer to a complete monolayer than in the process utilizing solely water.

The refractive index at 580 nm was 2.06 for films grown at 150 °C. Increasing the deposition temperature to 250 °C increased the refractive index to 2.21. The highest refractive index, 2.27, was obtained by the H_2O−Ta−O pulsing sequence at 250 °C, whereas the Ta−H_2O−O pulsing sequence resulted in refractive index of 2.06. The latter is close to what was obtained also in this work and reported earlier for the thermally activated tantalum ethoxide−water process at similar temperatures.[13]

The tantalum oxide films deposited without the additional water pulse were somewhat oxygen-rich at both 150 and 250 °C deposition temperatures (Table 2). Increasing the deposition temperature from 150 to 250 °C, however, decreased the impurity amounts considerably and made the film nearly stoichiometric. The incorporation of water into the deposition process did not change the impurity contents dramatically, but changed the carbon-to-hydrogen ratio slightly, indicating a difference in the impurities present. The position of the water pulse in the deposition sequence had also some impact on the impurities. Pulsing water between the tantalum ethoxide and oxygen radical pulses, according to the Ta−H_2O−O sequence, resulted in 1.9 at % carbon and 2.8 at % hydrogen, whereas pulsing water before the tantalum ethoxide pulse according to the H_2O−Ta−O sequence resulted in 1.2 at % carbon and 1.9 at % hydrogen. The C:H ratio in

(36) Kreissig, U.; Grigull, S.; Lange, K.; Nitzsche, P.; Schmidt, B. *Nucl. Instrum. Methods Phys. Res., Sect. B* **1998**, *136*−*138*, 674.
(37) Spaeth, C.; Richter, F.; Grigull, S.; Kreissig, U. *Nucl. Instrum. Methods Phys. Res., Sect. B* **1998**, *140*, 243.
(38) Ziegler, J. F.; Biersack, J. P.; Littmark, U. *The Stopping and Range of Ions in Solids, Vol. 1*; Pergamon Press: New York, 1985.
(39) Ylilammi, M.; Ranta-aho, T. *Thin Solid Films* **1993**, *232*, 56.

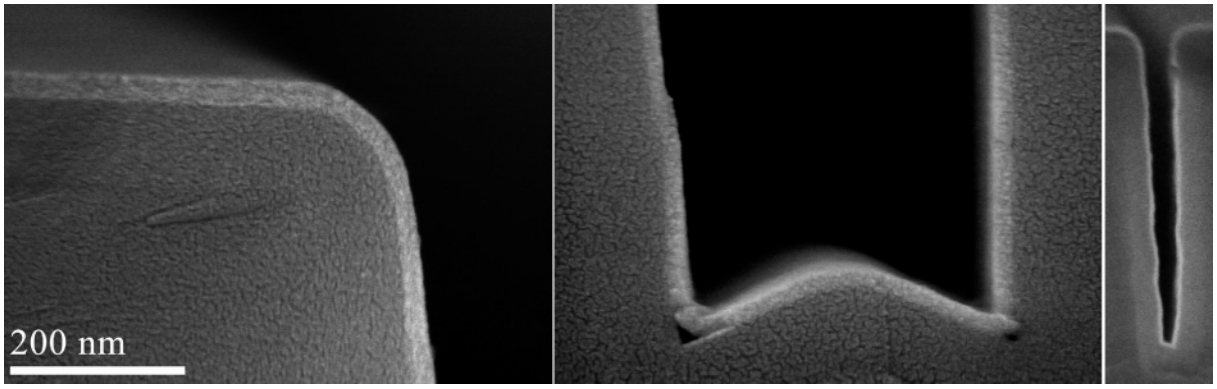

Figure 2. Cross-sectional SEM images of a 40 nm Ta_2O_5 grown on patterned trench structures with a 5:1 aspect ratio (left and middle) and a 11:1 aspect ratio (right). The images show texture from Pd/Pt coating. The width of the right image is 500 nm.

Table 2. Film Composition According to ERDA (Ta:O ratio is calculated from the bulk composition; uncertainty for each value is shown in parentheses)

	composition (at %)				
process	Ta:O	Ta	O	C	H
Ta−O, 150 °C	2:5.6	21.6 (±0.5)	60.7 (±2.2)	3.3 (±0.3)	13.8 (±0.4)
Ta−O, 250 °C	2:5.1	25.2 (±.6)	72.1(±2.7)	0.6 (±0.1)	2.1 (±0.1)
H_2O−Ta−O, 250 °C	2:5.0	27.8 (±0.6)	69.1 (±2.2)	1.2 (±0.15)	1.9 (±0.1)
Ta−H_2O−O, 250 °C	2:5.2	26.8 (±0.6)	68.5 (±2.7)	1.9 (±0.25)	2.8 (±0.1)

the film deposited at 250 °C with the Ta−O sequence is close to 2:5, indicating the possibility of left-over ethoxide ligands, C_2H_5O. Thus, the excess oxygen is also likely in the ethoxide residues. However, the C:H ratio in the films deposited using the additional water pulse is approximately 2:3, which indicates that the films may contain other impurities besides ethoxide ligands.

The density of the films varied with deposition temperature and was slightly affected by the incorporation of additional water pulses (Figure 3). The film density was 7.1 g/cm^3 for the film deposited at 150 °C and increased to 7.6 g/cm^3 for films deposited at 250 °C. The density was slightly lower for the H_2O−Ta−O sequencing, 7.2 g/cm^3. The film roughness was also analyzed from XRR: the rms roughness was 1.4 nm for a 90 nm thick film deposited at 250 °C with the Ta−O and increased to 2.6 nm with the H_2O−Ta−O sequencing. Normally an increase in roughness indicates an increase in the degree of crystallinity, but no changes were observed, at least with XRD. Therefore, differences in nucleation density and subsequently agglomeration are a more likely explanation for the different roughnesses.

The dielectric constant increased with the deposition temperature. The dielectric constants were 28 and 36 for

Table 3. Electrical Properties of the Films Grown at 150 and 250 °C on Platinum with Different Sequencings

sequence	deposition T (°C)	leakage current density at 1 MV/cm (μA/cm^2)	dielectric constant (ϵ)
Ta−O	150	0.01	28
Ta−O	250	0.01	36
H_2O−Ta−O	250	480	31
Ta−H_2O−O	250	0.05	34

about 110 nm thick films deposited on platinum at 150 and 250 °C. The leakage current density at 1 MV/cm electric field was 1×10^{-8} A/cm^2 for both films (Figure 4). This value is likely limited by the simple measurement setup, with the actual leakage current density being lower. For comparison, the dielectric constant obtained with the thermally activated tantalum ethoxide−water process was only 21 at 250 °C deposition temperature, and the leakage current at 1 MV/cm electric field was 4×10^{-3} A/cm^2.[13] Adding water to the pulsing sequence at 250 °C decreased the dielectric constant and increased the leakage currents, with both H_2O−Ta−O and Ta−H_2O−O pulsing sequences (Table 3 and Figure 4). The deterioration of the electrical properties was most severe with the H_2O−Ta−O sequence, which is contrary to the low impurity amounts. The electrical proper-

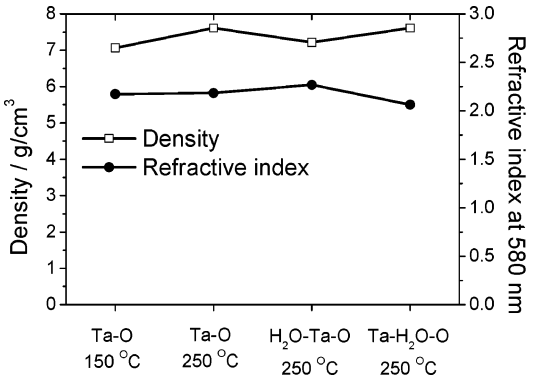

Figure 3. Film density and refractive index for different deposition sequences.

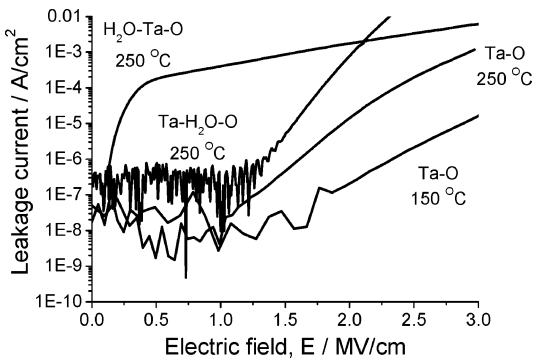

Figure 4. Leakage current densities as a function of applied field for tantalum oxide films grown on platinum with different deposition sequences at 150 and 250 °C.

ties were, however, still better than what was obtained with the thermally activated tantalum ethoxide−water process at 250 °C. The leakage current densities at 1 MV/cm were 4.5 × 10^{-4} A/cm^2 and 5 × 10^{-8} A/cm^2, and the dielectric constants 31 and 34 for the H_2O−Ta−O and Ta−H_2O−O sequences. Thus, it would seem that the main obstacle in obtaining good electrical properties with the thermally activated tantalum ethoxide−water process is related to the first half-reaction, i.e., the step where tantalum ethoxide adsorbs on the hydroxyl-covered surface. This is reflected by the poorer electrical properties obtained with the H_2O−Ta−O sequence. On the other hand, the slow growth rate obtained with the Ta−H_2O−O sequence approaches the value obtained with the thermally activated tantalum ethoxide−water process. This, in turn, suggests that the growth rate is determined by the second half-reaction, the reaction of water with the adsorbed tantalum ethoxide and possibly other adsorbed species. It would seem that the electrical properties and growth rate are determined by different steps in the tantalum ethoxide−water reaction.

The difference in growth rates obtained with the different sequences (Table 1) is interesting and seems to indicate a difference in growth mechanism, especially between the water- and oxygen-radical-based processes. In the water-based process, the ligands are released in a reaction of tantalum ethoxide and surface hydroxyl groups:[40]

$$Ta(OC_2H_5)_5(g) + (5 - x)\ {-}OH(ads) \rightarrow Ta(OC_2H_5)_x(ads) + (5 - x)\ C_2H_5OH$$

The hydroxyl groups are formed on the surface in a reaction between surface-bound ethoxide ligands and H_2O

$$-OC_2H_5(ads) + H_2O(g) \rightarrow -OH(ads) + C_2H_5OH(g)$$

$Ta(OC_2H_5)_x$ adsorption density is expected to determine the growth rate per cycle.[14] This density is in turn likely to depend on the *x*, i.e., how many ligands are left bound with Ta in $Ta(OC_2H_5)_x$(ads). In READL, the exact growth mechanism is not known. One possibility is that after the oxygen radical pulse, the surface is left clean, without any functional groups. Another possibility is that the byproducts from the reaction between ethoxide ligands and oxygen radicals, most likely CO_x and H_2O, are readsorbed and form functional sites, in particular OH groups. If this is the case, the higher growth rates in the Ta−O and H_2O−Ta−O processes seem to indicate that the OH coverage formed when $Ta(OH)_x$(ads) reacts with oxygen radicals is higher than that formed in reactions with water. Finally, a bare Ta_2O_5 surface may catalyze the partial decomposition of Ta-$(OC_2H_5)_5$ among other reactions, as long as it is not covered by any decomposition products or OH groups.[41,42] As oxygen radicals are used during the deposition, there may be sufficient UV emission from the recombination processes to activate photocatalytic reactions of the surface tantalate species.

Conclusion

Tantalum oxide was grown at 150 and 250 °C from tantalum ethoxide and oxygen radicals on several substrate materials. Water was used as an additional reactant in some experiments. The film growth occurred in the ALD mode. The films had good electrical and optical properties and grew conformally. The films were relatively pure, especially when compared to films deposited with water-based thermal ALD processes at similar temperatures. The addition of a water pulse before the tantalum precursor pulse, according to the H_2O−Ta−O sequence, increased the refractive index but increased the impurity contents slightly. The addition of a water pulse after the tantalum ethoxide pulse, according to the Ta−H_2O−O sequence, decreased the growth rate and refractive index significantly and resulted in poorer electrical properties.

The exact chemical nature of the surface onto which tantalum ethoxide chemisorbs remains to be studied. On the basis of our results, it seems obvious that the surfaces differ significantly in different sequencing of the precursors, which is reflected, for example, on the growth rates. Also, the effect of postdeposition annealing on these films remains to be studied. On the other hand, the electrical properties of the films grown at both 150 and 250 °C are sufficient for many purposes, even without high temperature annealing.

Acknowledgment. The Academy of Finland supported this work financially through Project 203291. We thank Mr. Teemu Alaranta for conducting part of the electrical measurements.

CM0626482

(40) Rahtu, A.; Kukli, K.; Ritala, M. *Chem. Mater.* **2001**, *13*, 817.
(41) Tanaka, T.; Nojima, H.; Yamamoto, T.; Takenaka, S.; Funabiki, T.; Yoshida, S. *Phys. Chem. Chem. Phys.* **1999**, *1*, 5235.
(42) Chen, Y.; Fierro, J. L. G.; Tanaka, T.; Wachs, I. E. *J. Phys. Chem. B* **2003**, *107*, 5243.